# Thermodynamic Perfomance Comparison of Working Fluids Based on Organic Rankine Cycle in Waste Power Plants

*Kornelis* Kopong Ola1[1,3] *Joko* Waluyo[2,*] *Cahyadi*[3], *Lina* Agustina[3]

[1] Magister of System Engineering, Faculty of Engineering, Gadjah Mada University Indonesia
[2] Magister of System Engineering, Faculty of Engineering, Gadjah Mada University Indonesia
[3] National Research and Innovation Agency Indonesia

**Abstract.** The use of alternative fuels, other than fossil fuels, is an interesting issue for power generation today. The power plant option used is a waste power plant that utilizes the heat exhausted from the garbage. The study investigate a thermodynamic analysis four working fluids at a power plant based on the organic Rankine cycle (ORC) using waste heat that comes out of an incinerator located in Soreang Bandung. The working fluids are R123, n-butane, n-pentane, and R245fa. The temperature of the heat vapor coming out of the incinerator is 450 °C with a heat vapor flow of 3 kg/s. Consideration Thermodynamic analysis was performed with a turbine inlet temperature of 130 °C because one of the fluids was already close to the critical temperature. (EES). Based on the thermodynamic analysis of each fluid, R123 produced the most power (91.22 kW), whereas R254fa provided the lowest power (87.92 kW). The plant exhibited the maximum power consumption at 25.93 kW and the lowest at 19.51 kW. The n-pentane fluid demonstrated the highest thermal efficiency at 8.86%, while the n-butane fluid had the lowest thermal efficiency at 7.94%.
Keywords: ORC, Thermodynamic Comparison, Energy Power Plant, Working Fluid

## 1 Introduction

Presently, power plants are utilizing low-enthalpy heat sources as a means to decrease their dependence on fossil fuels. Power plants utilizing environmentally friendly technology offer significant potential for mitigating CO2 emissions. When waste is effectively controlled, it can be utilized as a cost-efficient source for producing power, due to technological breakthroughs such as the implementation of Organic Rankine Cycle technology (ORC). When the temperature of the is still high, it has the ability to transfer heat to other working fluids like n-pentane or n-butane. This heat transfer allows the vapor produced by these fluids to be used for generating power. In addition to the ORC system utilized in waste power plants, there exist alternative technologies that facilitate the conversion of waste into electrical energy. Within a waste-to-energy treatment system, the incinerator room combusts waste

* Corresponding author: jokowaluyo@ugm.ac.id

materials, resulting in the heating of boilers containing water. This process leads to the production of steam, which is utilized to directly power the turbine and generate energy [1, 2]. In addition, the processes of gasification and pyrolysis utilize waste heat to generate syngas and biofuel, respectively. Generators utilize syngas as a fuel source for the purpose of producing electricity [3]. Digesters not only transform waste's thermal energy, but also process it to generate biogas, which may be used as fuel for producing electricity [4].

Several researches have investigated the utilization of the Organic Rankine Cycle (ORC) system for power generation in power plants. These studies have focused on using brine, which has a composition dominated by water, as a heat source. Additionally, these studies have compared the performance of brine with other fluids. Aside from the geothermal energy derived from the earth's heat, there are other power plants that utilize waste heat from sources such as diesel [7], solar [8, 9], and biomass [10]. These power plants heat other fluids to generate electricity for areas with limited resources. The ORC technology is an appropriate method for converting low-enthalpy heat sources into electric energy using other heat sources, such as brine. This technology can utilize n-pentane as the working fluid and has been successfully implemented with a producing capacity of 2 kW [11] and a larger capacity of 500 kW [12]. Additionally, in laboratory-scale testing, alternative work fluids such as R245fa and R123 have been used [13].

This study examined the thermodynamics of waste power plants equipped with the ORC system. The investigation focused on the waste incineration results obtained from Soreang Bandung. In this system, the heat generated from the exhaust of incinerators is utilized as a heat source. The study considered four different types of working fluids: n-pentane, n-butane, R123, and R245fa. The temperature of the gas emitted from the incinerator is around 450 °C, and it has a mass flow rate of 3 kg/s.

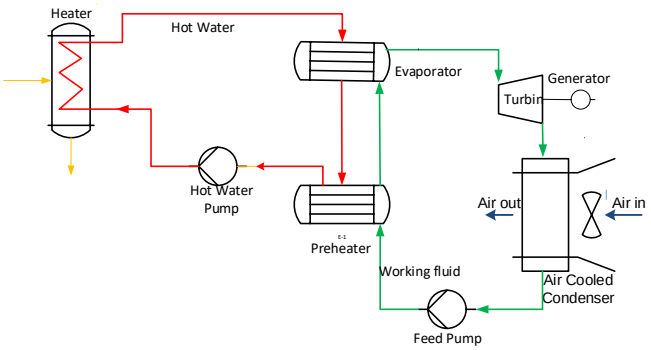


**Fig. 1.** Process flow diagram of waste to energy power plant

Figure 1 depicts the waste heat utilization process for the power plant ORC system, in which waste heat is utilized to heat cold water by feeding it into the heater. The heater transforms low-temperature water into high-temperature water, so raising the temperature and causing the working fluids in the preheater and evaporator to heat up and turn into vapor. The vaporized working fluid is thereafter directed towards turbines that are connected to generators in order to generate power. The water-cooled condenser in an air conditioning system condenses the expansion fluid that comes out of the turbine, pumps it back into the heat exchanger, and reuses it to power the turbine once more. Due to the flammability and high toxicity of working fluids, it is necessary for the system to operate in closed cycles. The turbine must be securely sealed to prevent any leaking.

## 2 Research Methodology

Figure 2 depicts the process diagram of the thermodynamic cycle ORC (2a) and the p-h diagram of the ORC cycle (2b). The working fluid being pumped from the tank, increasing its pressure isentropically (3-4), then heated in the preheater and evaporated in the evaporator isobarically (4-1). The vapor exiting the evaporator can be in a saturated state (1). The vapor is then expanded in the turbine isentropically, converting thermal energy into mechanical energy (1-2). The vapor leaving the turbine is condensed in the condenser isobarically (2-3), and the process repeats, forming a closed ORC cycle. The heating fluid used is water, which is pumped from the tank to the heater (7-8) and exits the heater to heat the working fluid in the preheater and evaporator (5-6).

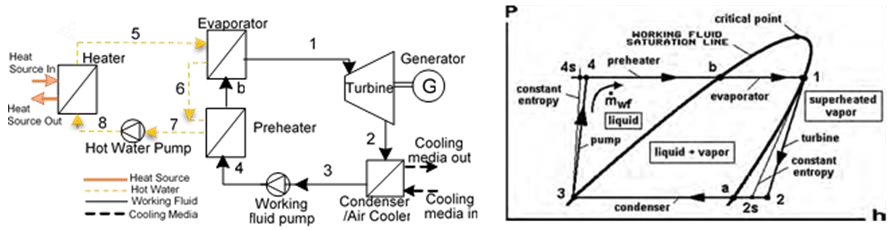


(a) (b)

**Fig. 2**. ORC process thermodynamic cycle (a) and P-h diagram (b) [14]

The thermodynamic process calculation as in Figure 2 uses the following equation:

Turbine power

$$\dot{W}_t = \dot{m}_{wf}(h_1 - h_2) = \dot{m}_{wf}\eta_t(h_1 - h_{2s}) \quad (1)$$

Energy balance in the Condenser/Air Cooler

$$\dot{m}_{Ac}(h_{out} - h_{in}) = \dot{m}_{wf}(h_2 - h_3) \quad (2)$$

Cooler /Condenser Load

$$\dot{Q_{ac}} = \dot{m}_{wf}(h_2 - h_3) \quad (3)$$

Working fluid feed pump power

$$\dot{W_p} = \dot{m}_{wf}(h_4 - h_3) = \dot{m}_{wf}(h_{4s} - h_3)/\eta_p \quad (4)$$

Energy balance in the evaporator

$$\dot{m}_{hw}Cp_{hw}(T_5 - T_6) = \dot{m}_{wf}(h_1 - h_b) \quad (5)$$

Evaporator Load

$$\dot{Q_{eva}} = \dot{m}_{wf}(h_1 - h_b) \quad (6)$$

Energy balance in the Preheater

$$\dot{m}_{hw}Cp_{hw}(T_6 - T_7) = \dot{m}_{wf}(h_b - h_1) \quad (7)$$

Preheater Load

$$\dot{Q_{pre}} = \dot{m}_{wf}(h_b - h_1) \quad (8)$$

Heat input to the system

$$\dot{Q}_{in} = \dot{m}_{hw}(h_5 - h_7) = \dot{m}_{wf}(h_1 - h_4) \quad (9)$$

Hot water Pump Power

$$\dot{W_{hw}} = \dot{m}_{wf}(h_8 - h_7)/\eta_p \quad (10)$$

Air Cooled Condenser Motor Power

$$\dot{W_{ac}} = \dot{m}_a(h_{out} - h_{in})/\eta_m \quad (11)$$

Electric power produced by the generato

$$W_g = \eta_t x \eta_g x W_t \quad (12)$$

Nett Power generated

$$W_{nett} = W_g - W_p - W_{hw} - W_{ac} \quad (13)$$

Overall cycle analysis

$$\eta_{th} = \frac{W_{net}}{\dot{Q}_{in}} \quad (14)$$

Equations (1) and (14) are used to calculate thermodynamic heat and balance. The computation is based on the assumption of waste heat field conditions. Table 1 displays the temperature conditions and rate at which heat is released from the waste incinerator. Table 2 presents the calculation references that include hot water temperature, hot water mass flow, pump efficiency, ambient pressure and temperature, turbine isentropic efficiency, turbin inlet temperature and generator efficiency for comparing the working fluid performance.

**Table 1**. Incinerator data

| Parameter | Value |
|---|---|
| Waste heat temperature | 450 $^0$C |
| Waste heat mass flow | 3 kg/s |

**Table 2**. Calculation reference

| | |
|---|---|
| Hot water temperature | 160 $^0$C |
| Hot water mass flow rate | 3,14 kg/s |
| Pump efficiency | 75% |
| Motor efficiency | 75% |
| Ambient pressure | 1 bar |
| Ambient temperature | 27 $^0$C |
| Turbine isentropic efficiency | 75 % |
| Turbine inlet temperature | 130 $^0$C |
| Generator efficiency | 90 % |

Table 3 below shows the differences in the physical properties of the four simulated working fluids.

**Table 3**. Working Fluid Properties for ORC [14,15]

| Fluid | Formula | Molecular weight | $T_{critical}$ ($^0$C) | $P_{critical}$ (bar) | $P_{Cond}$ at 38 $^o$C (bar ) | Toxicity | Flam | GWP/ ODP |
|---|---|---|---|---|---|---|---|---|
| n-butane | $C_4H_{10}$ | 58.1 | 152 | 37.5 | 3.5 | Low | High | 3/0 |
| n-pentane | $C_5H_{12}$ | 72.2 | 196,6 | 33.3 | 1.0 | Low | High | 3/0 |
| R-123 | $C_2HCl_2F_3$ | 152.8 | 183,8 | 36.1 | 1.2 | High | Non | 77/0 |
| R-245fa | $C_3H_3F_3$ | 134 | 154,1 | 43.7 | 2.3 | Medium | Non | 1030/0 |

For the temperature parameters of the turbine inlet and the pressure of the condenser/water cooler, use the reference in Table 3. The temperature of the inlet is limited to 130 °C since the fluid n-butane and R245fa at that temperature are already close to the critical temperature and the condition at which the vapor entering the turbine is saturated vapor.
Table 4 provides a comprehensive overview of the various factors that need to be taken into account when selecting the working fluids, in addition to thermodynamic considerations. their characteristics such as toxicity, flammability, ozone depletion potential (ODP), and global warming potential (GWP).

## 3 Results and Discussions

The calculations using engineering equation solver simulation (EES) results were based on equations (1) to (14), using a hot water temperature of 160 °C and a flow rate of 3.14 kg/s. The turbine's inlet temperature is limited to 130°C at saturated steam conditions due to the fact that the fluids n-butane and R245 fa are nearing their critical temperatures at that specific temperature. When the temperature rises, it leads to a mixture of liquid and steam entering the turbine, which causes the turbine's blades to be damaged by water particles. Presented here are simulated P-h and T-s diagrams for fluids derived from the four distinct fluid types.

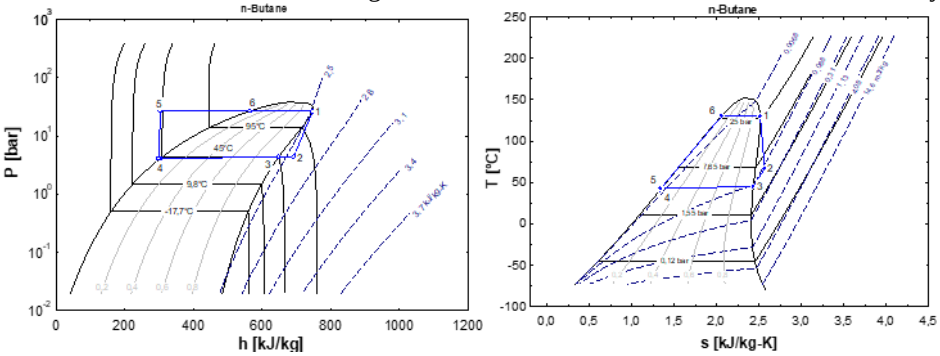


**Fig. 3**. P-h and T-s diagram of n-butane

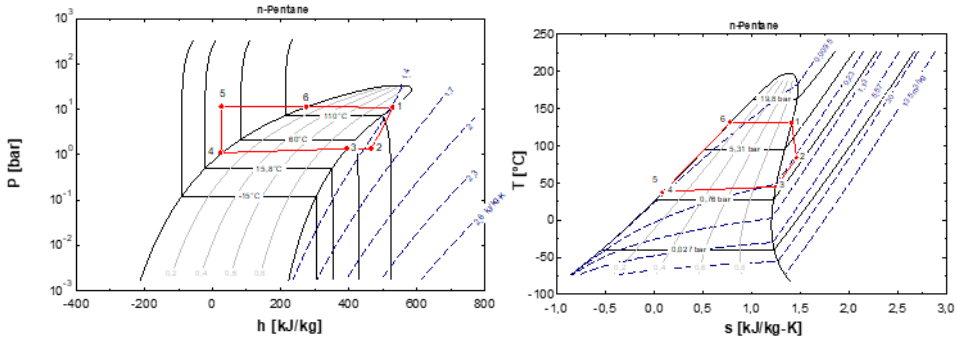


**Fig. 4**. P-h and T-s diagram of n-pentane

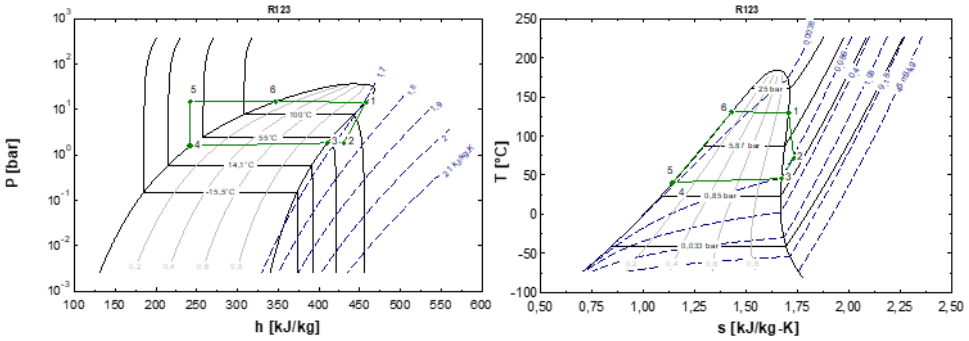


**Fig. 5**. P-h and T-s diagram of R123

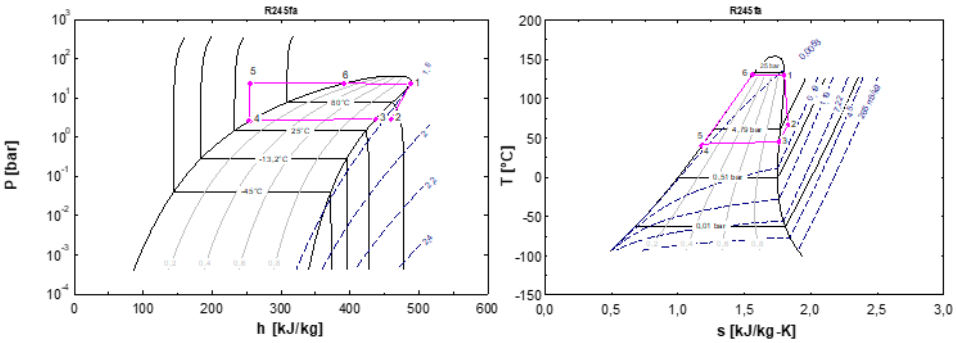


**Fig. 6**. P-h and T-s diagram of R245fa

Figures 3-6 show diagrams p-h and T-s that depict the simulation findings of the work fluid units n-butane, n-pentane, R123, and R245fa. At points 1-2, the process involves a turbine expansion that maintains constant entropy. Point 2-3-4 signifies the release of heat at constant pressure in the water cooler or condenser. Point 5-6-1 represents the supply of heat at constant pressure in the preheaters and evaporators. The T-s diagram assumes that the temperature at the evaporator's outlet is the same as the temperature at the turbine's inlet, indicating that there is no temperature increase. The simulated working fluid, which is both 75% turbine efficiency and dry, superheats upon expansion in the turbine, eliminating the need for additional heating at the turbine's inlet. The T-s diagram curve for hydrocarbon and halocarbon fluids exhibits retrograde behaviour, in contrast to water, which follows a vertically straight path [16, 17]. Furthermore, concerns about fluid droplets on the turbine's blades have diminished.

Table 4 shows the results of the T-s diagram, which compares several parameters in Figures 3-6.

**Table 4**. Comparison of pressure and temperature of the simulated working fluids

| Fluid | Turbine inlet pressure | Turbine outlet temperature |
|---|---|---|
| | (bar) | $^0$C |
| n-pentane | 11.01 | 83.24 |
| n-butane | 26.32 | 65.05 |
| R123 | 14.61 | 71.82 |
| R245fa | 23.39 | 66.89 |

Table 4 shows that the highest turbine inlet pressure is n-butane fluid and the lowest is n-pentane fluid. The high inlet pressure of the turbine will affect cost of the material used. The higher the pressure the thicker the equipment material used. For the turbine exit temperature of the four working fluids, it is still dry fluid with superheated conditions so that it can still be utilized again by using a recuperator tool to increase the efficiency of the power plant.[18]

To determine the power and inlet pressure at each temperature change in the turbine's inlet, analyse and compare the characteristics of the four fluids depicted in Figure 8.

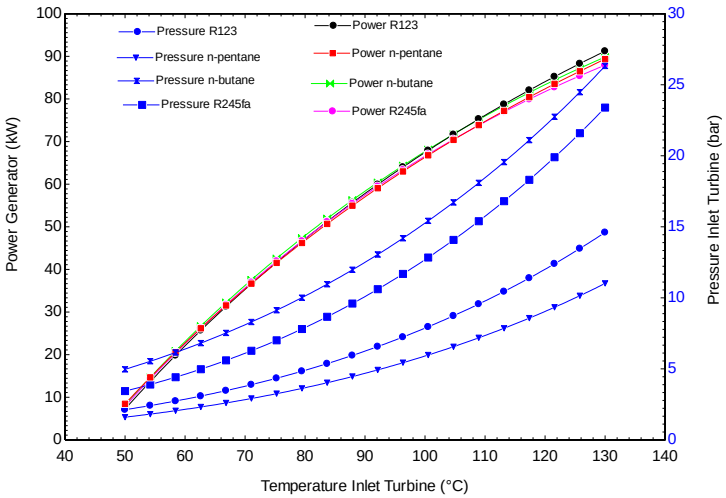


**Fig. 7**. Generator power and inlet pressure versus turbine inlet temperature

Figure 7 exhibits that a turbine with high inlet pressure does not consistently produce a high-power generator. However, it does create greater power as the temperature rises. The maximum power output is achieved at a temperature of 130 °C.

The power generator produced by the power plant has a portion of its energy allocated for internal use, such as powering pumps and air cooler. Table 5 demonstrates the magnitude of the power.

**Table 5**. Power consumption for the plant

| Fluid | working fluid mass flow rate | Power Consumption | Nett Power | Power Generated | Thermal Efficiency |
|---|---|---|---|---|---|
| | (kg/s ) | (kW) | (kW) | (kW) | (%) |
| n-pentane | 1.5 | 19.51 | 69.85 | 89.36 | 8.86 |
| n-butane | 1.82 | 25.93 | 63.9 | 89.82 | 7.94 |
| R123 | 3.73 | 20.55 | 70.66 | 91.22 | 8.78 |
| R245fa | 3.46 | 23.53 | 64.93 | 87.92 | 8 |

Equation (5) utilizes heat and balance to calculate the mass flow rate of the working fluid in Table 4, whereas equations 1 and 12 determine the functions of the turbine and generator. The n-butane fluid has the highest power consumption because of its characteristics at the highest inlet pressure of the turbine. This means that a high working fluid pump power is required. On the other hand, the n-pentane has the lowest power consumption due to its small inlet turbine pressure, resulting in a low power requirement for the pump. It is noted that thermal efficiency in ORCs tends to be on the lower side, as indicated by several studies on ORCs with different working fluids, which report averages ranging from 5.5% to 25% [19].

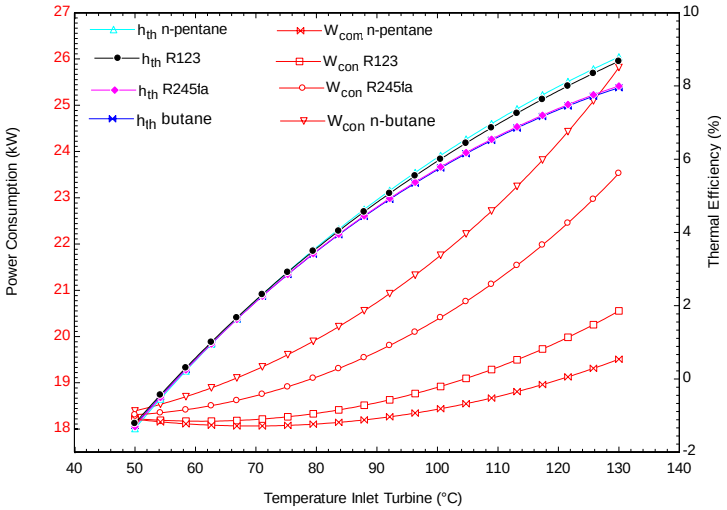


**Fig. 8.** Power consumption and thermal efficiency against inlet turbine temperature

Figure 8 illustrates the variations in power consumption and thermal efficiency in relation to the turbine's temperature inlet. A direct relationship between power consumption and thermal efficiency: as power consumption decreases, thermal efficiency increases is also indicated in that Figure.

## 4 Conclusions

Based on the thermodynamic analysis results, it is evident that R123 generates the highest power output at 91.22 kW, whereas R254fa produces the lowest power output at 87.92 kW. The plant's largest power consumption comes from the n-butane fluid, which is at 25.93 kW. On the other hand, the lowest power consumption is from the n-pentane fluid, which is at 19.51 kW. In terms of thermal efficiency, the highest is achieved by the n-pentane fluid at 8.86%, while the lowest is from the n-butane fluid at 7.94%. The working fluid N-pentane, specifically n-butane, possesses flammable properties, while R123 and R245fa are non-flammable. The toxicity levels of the fluid R123 and R245fa are high and moderate, respectively, whereas n-pentane and n-butane do not pose any toxicity risks. The GWP/ODP values of n-butane and n-pentane are 20/0, while R123 and R245fa have GWP/ODP values of 77/0 and 1030/0, respectively.

The author expressed gratitude to the BRIN (National Research and Innovation Agency) for their support of this research.

## Nomenclature

| | | | |
|---|---|---|---|
| $Cp_{hw}$ | Specific heat of hot water, kJ/kg | $h_b$ | Enthalpy at preheater outlet, kJ/kg |
| $h_1$ | Actual working fluid enthalpy at turbine inlet/evaporator outlet, kJ/kg | $\dot{m}_{hw}$ | Hot water mass flowrate, kg/s |
| $h_2$ | Actual working fluid enthalpy at turbine outlet, kJ/kg | $\dot{m}_{ac}$ | Cooling air mass flowrate, kg/s |
| $\eta_t$ | Turbine isentropic efficiency, % | $\dot{m}_{wf}$ | Working fluid mass flow rate, kg/s |
| $h_{2s}$ | Working fluid enthalpy at turbine outlet, in isentropic condition, kJ/kg | $\dot{Q}_{ac}$ | Condenser /Air cooler load, kW |

| | | | |
|---|---|---|---|
| $h_3$ | Working fluid enthalpy at condenser/air cooler outlet, kJ/kg | $\dot{Q}_{eva}$ | Evaporator load, kW |
| $h_5$ | Hot water enthalpy at evaporator inlet, kJ/kg | $\dot{Q}_{pre}$ | Preheater load, kW |
| $h_7$ | Hot water enthalpy at preheater outlet, kJ/kg | $Q_{in}$ | Heat input, kW |
| $h_4$ | Working fluid enthalpy at preheater inlet, kJ/kg | $T_5$ | Temperature of hot water at evaporator inlet, °C |
| $h_{in}$ | Air enthalpy inlet at air cooler, kJ/kg | $T_7$ | Temperature of hot water at preheater outlet, °C |
| $h_{out}$ | Air enthalpy outlet at air cooler, kJ/kg | $W_g$ | Generator power, kW |
| $h_{out}$ | Cooling air enthalpy at condenser/air cooler outlet, kJ/kg | $W_{hw}$ | Hot water pump power, kW |
| $h_{in}$ | Cooling air enthalpy at condenser/air cooler inlet, kJ/kg | $W_{ac}$ | Air cooled condenser motor power, kW |
| $h_4$ | Actual working fluid enthalpy at pump outlet, kJ/kg | $W_{net}$ | Net power output, kW |
| $h_{4s}$ | Working fluid enthalpy at pump outlet, at isentropic condition, kJ/kg | $W_{com}$ | Power consumption, kW |
| $T_6$ | Temperature hot water at evaporator outlet/ at preheater inlet, °C | $\eta_{th}$ | Thermal efficiency, % |

## References

1. N.P Agatha, A.A Harvan, F.R Prasetya, *Examining waste-to-energy technology potential through the pilot project of Bantargebang Waste-to-Energy Power Plant*, in Proceedings of The E3S Web of Conferences 485, (2024)
2. UNEP, Waste-to-Energy: Considerations for Informed Decision-Making (2019)
3. M.M. Hasan, M.G. Rasul, M.M.K. Khan, N. Ashwath, M.I. Jahirul, Renewable and Sustainable Energy Reviews**, 145,** 11107 (2021)
4. T. Ariyanto, R.B. Cahyono, A. Vente, S. Mattheij, R. Millati, Sarto, M.J. Taherzadeh, S. Syamsiah, International Journal of Technology **8**, 1385-1392 (201
5. Franco, M. Villani, Geothermics, **38** (4), 379-391 (2009)
6. M.D. Surindra, W. Caesarendra, T. Prasetyo, T.M.I. Mahlia, Taufik, Processes, **7** (2), 113 (2019)
7. J. Rijpkema , O. Erlandsson, S.B. Andersson, K. Munch, Energy, **238**, 121698 (2022)
8. Kumara, S.K. Shuklab, Procedia Technology, **23**, 454-463(2016)
9. T.F. Bertand, G. Papadakis, G. Lambrinos, A. Frangoudakis, Applied Thermal Engineering, **29** (11-12), 2468 (2010)
10. H. Ismail, A.A. Aziz, R.H. Rasih, N. Jenal, Z. Michael, A. Roslan, Journal of Advanced Research in Applied Sciences and Engineering Technology, **4**(1), 29-46(2016)
11. B.T. Prasetyo, S. Himawan, Suyanto, T. Surana, L. Agustina, Y. Yasser, M.D. Trisno, *Design and Testing of n-Pentane Turbine for 2 kW Model of Binary Cycle Power Plant*, In Proceedings World Geothermal Congress, 25 – 28 April 2010, Bali, Indonesia (2011)
12. S. Frick, S. Kranz, G. Kupfermann, A. Saadat, E. Huenges, Geotherm Energy, **7** (30) (2019)
13. M. Kukurugyová, G.G. Akkurt, J. Nalevanková, R. Dzurňák, *Comparison of working fluids fororcgeothermal power plant ďurkov*, in Proceedings of

eConference of Doctoral Students and Young Researcher, ISeC, 20 – 24 July 2015, Bratislava, Slovakia (2015)
14. R. DiPippo, Geothermal power plants: principles, applications, case studies and environmental impact, (2012)
15. D.H. Kihara, P.S. Fukunaga, Working fluid selection and preliminary heat exchanger design for a Rankine cycle geothermal power plant (1975)
16. B.F. Tchanche, G. Lambrinos, A. Frangoudakis, G. Papadakis, Renewable and Sustainable Energy Reviews,15 (8), 3963-3979 (2011)
17. B.A. Fakeye, S.O. Oyedepo, IOP Conf. Ser.: Mater. Sci. Eng. **413**, 012019 (2018)
18. S. Ependi, T.B. Nur, IOP Conf. Ser.: Mater. Sci. Eng. **309,** 012055 (2018)
19. J.C.J. García, A. Ruiz, A. Reyes, W. Rivera, Processes, **11**(7):1982 (2023)